Available online at www.sciencedirect.com
SCIENCE DIRECT®
Journal of the European Ceramic Society 25 (2005) 243–249
www.elsevier.com/locate/jeurceramsoc

Nanodevices that explore the synergies between PDCs and carbon nanotubes

S.R. Shah*, R. Raj

Department of Mechanical Engineering, University of Colorado, Boulder, CO 80309-0427, USA

Abstract

There is now good evidence that carbon nanotubes can be coated uniformly with a very thin, perhaps even a monolayer, of a polymer-derived ceramic (SiCN) by a simple process of soaking the nanotube surfaces with the liquid precursor followed by pyrolysis. The ceramic coating bonds the nanotubes to one another, which suppresses time-dependent creep that is present without the ceramic bonding. In this article we address the influence of the ceramic coating on two functional properties of carbon nanotube structures—the electrolytic supercapacitance and electrochemico-mechanical actuation. The results, when expressed as the equivalent surface capacitance of carbon sheets, are quite unexpected. The ceramic coating appears to increase the surface capacitance of the nanotube structure. The actuation induced by capacitive charging is also shown to be somewhat enhanced, although the principal influence of the coating is to suppress the drift of the actuation seen in unbonded carbon nanotube structures. It is inferred that the thickness of the SiCN coating amounts to approximately one monolayer of coverage of the nanotubes.

Keywords: SiCN; Nanotubes; Capacitive charging

1. Introduction

The fundamental origin of a synergy between polymer-derived ceramics and carbon nanotubes lies in a recent finding that polysilazane, *the liquid organic precursor for silicon carbonitride*, SiCN,[1] wets and, therefore, completely coats the surfaces of the nanotubes. Thus, a pervasive, thin coating of SiCN on an entire nanotube structure can be created by placing a drop of the precursor on a carbon nanotube structure, which is immediately drawn in by forces of surface tension. This organic coating is converted into the ceramic by controlled pyrolysis.[2] New results, presented here, suggest that the coatings made in this simple way have an average thickness of about one monolayer.

Carbon nanotube paper is an example of a nanotube structure, which is easily fabricated, from a liquid emulsion, or ink, of carbon nanotubes, by a filter-pressing process.[3] The paper can have multifunctional properties which derive on the one hand from the large surface area of the paper, which ranges from a few hundred to a thousand m^2 per gram, and on the other hand from the fact that the sharp curvature of the nanotubes creates a high degree of surface activity of the carbon atoms. Two properties of the nanotube paper have been of interest: (a) the electrolytic supercapacitance[4] and (b) mechanical actuation produced by a change in the lattice parameter of the nanotubes when charge is injected into them in this way. The change in the lattice parameter is theorized to produce 9.6% strain for every electron per carbon atom injected into the nanotubes.[6] However, the random distribution of the tubes in the paper apparently produces actuation strain which is almost one hundred times smaller than this theoretical upper bound;[6] still, even though the detailed mechanism for this deficit is not entirely clear, the actuation strain is large enough to be easily measured, analyzed and studied.

In this article, we explore the synergies between SiCN and carbon nanotubes. The first kind of synergy is simply mechanical. The paper prepared by filter pressing exhibits significant creep deformation when loaded in tension, which makes the actuation strain unsustainable. The introduction of the ceramic bonding creates a more rigid structure, which es-

* Corresponding author.

0955-2219/$ – see front matter © 2004 Elsevier Ltd. All rights reserved.
doi:10.1016/j.jeurceramsoc.2004.08.006

Table 1
Physical and electrochemical properties of coated and uncoated samples

Sample	SiCN (wt.%)	ML_{SiCN} (monolayers)	BET (m^2/g)	σ (S/cm)	C_g (F/g)	C_a ($\mu F/cm^2$)	Actuation strain (%)	Strain range (%)
U	0	n/a	544	217	29	5.3	0.05	0.04–0.1
C1	10	0.06–0.08	490	183	22	4.5	0.07	0.07–0.1
C2	50	0.6–0.7	290	151	21	7.2	0.08	0.07–0.1

sentially eliminates the creep behavior in the nanotube paper. This work has been reported in Ref. [2].

The second kind of synergy is related to the double-layer electrolytic supercapacitance behavior of the nanotubes. When placed in an electrolyte of high ionic conductivity an electrochemical double layer is formed at the surface of the carbon nanotubes, which expresses as a supercapacitance. The magnitude of the capacitance is dependent on the width of the double layer (the Debye layer), which derives from the concentration profile of the ions on the electrolyte side, and the profile of the electrons on the carbon side of the interface. It was expected that the SiCN coating of the carbon nanotube surfaces would increase the width of the Debye layer and, therefore, significantly degrade the capacitance of the nanotube structure. However, experiments have shown that the capacitance is somewhat increased. *This remarkable result raises the possibility that the SiCN layer may itself incorporate graphene carbon like properties*. The fact that carbon in SiCN is known to be sp^2 bonded[7,8] certainly contributes to the credibility of such a notion.

The third kind of synergy is related to the electrochemical actuation in the nanotube paper. Intuition suggests that the coating would reduce the actuation strain; however, in this article we show that the strain in the coated paper is nearly the same as the strain achieved in the uncoated paper. These results and possible explanation for this behavior are presented.

The next section begins with presentation of the experimental findings. These results are grouped into four subsections: (i) materials preparation and characterization, (ii) measurement of the electronic conductivity, (iii) electrolytic capacitance, and (iv) mechanical actuation. Each set of experimental results is preceded by a brief description of the experimental method.

Detailed discussion of the results and their interpretation follows the presentation of the experimental findings.

2. Experimental methods and results

2.1. Materials preparation and characterization

The nanotube paper was made from purified HiPco nanotubes obtained from Carbon Nanotechnologies Inc., Houston, TX. These single-walled nanotubes are in the form of "Bucky pearls". The pearls are dispersed in water (50 mg CNT/L of DI water) by adding a non-ionic surfactant, Triton X-100 procured from Alfa Aesar, Chicago, IL, and ultrasonicating the mixture. The dispersion is filtered through 5 μm Teflon filter paper from Millipore Corporation, Bedford, MA. A "vacuum" pulled by a roughing pump on the other side of the filter accelerates the filtration process. The nanotubes deposited on the filter are further washed with methanol and water to remove as much surfactant as possible. The tubes deposited on the filter are then peeled off as a "paper". The nanotube paper is annealed at 1100 °C in flowing ultra high purity argon in an alumina muffle-tube furnace to burn off any remaining surfactant. This paper serves as the uncoated paper, identified as U, for the measurement of properties.

The SiCN coated papers (given the designations C1 and C2) were prepared as follows. Commercially available silazane-based precursor Polyureamethylvinylsilazane—

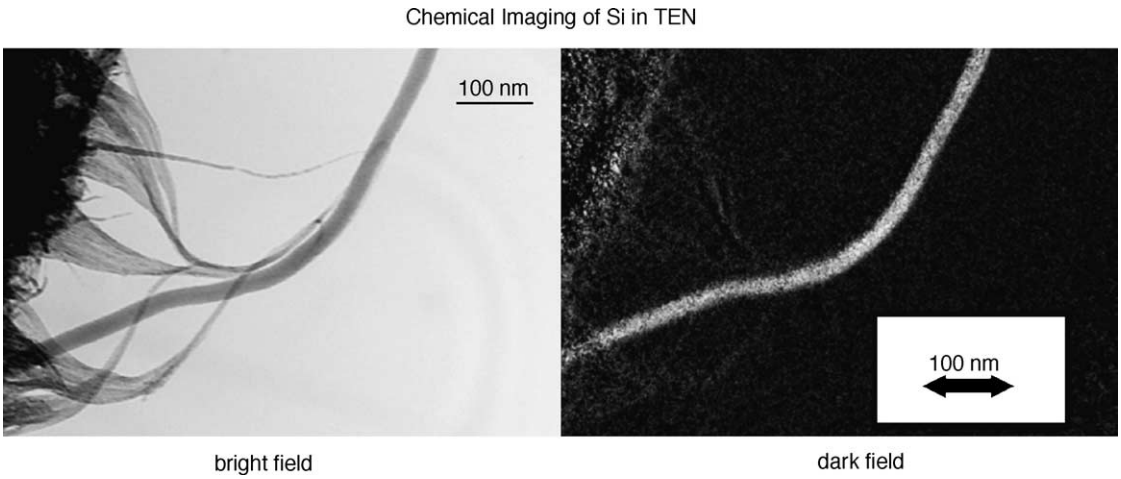

Fig. 1. The TEM micrograph on the left is a bright field image of a carbon nanotube bundle. The micrograph on the right is a dark field "chemical image" centered on the silicon filter, showing a uniform coverage with silicon (i.e., SiCN).

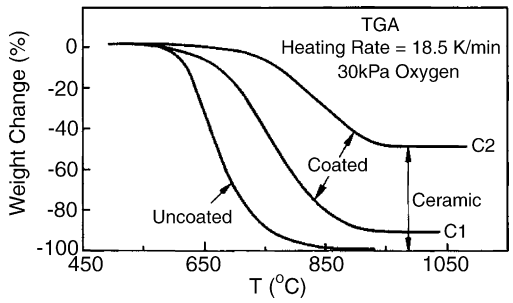

Fig. 2. TGA of uncoated and SiCN coated nanotube papers in 10 kPa oxygen pressure (ambient air) to determine the amount of SiCN in the coated nanotube papers.

Ceraset™-SN (Kion Corporation, Huntingdon Valley, PA) was used as the precursor of SiCN. Different concentrations of the Ceraset in acetone (2 and 10 vol.%) were used to vary the weight fraction of the SiCN coating. About 0.2 ml of solution was used to infiltrate 40 mm diameter nanotube paper. For smaller papers proportionately lower amount of liquid was used. The paper was left to dry in ambient air for about 15 min to allow the acetone to evaporate. Next, the paper was pyrolyzed to convert the polymer into the ceramic by heating in flowing argon at 1100 °C in an alumina muffle-tube furnace.

The coated and uncoated specimens were characterized in the following manner: (a) The distribution of SiCN on the carbon nanotube surfaces was characterized by energy-filtered transmission electron microscopy, which images the spatial distribution of the element Si. **(**b) The weight fraction of SiCN in the coated paper was determined by burning the paper in a thermo gravimetric analyzer (STA 409 from Netzsch Instruments, Paoli, PA) in ambient, flowing air. (c) The specific surface area of the papers was measured by BET analyzer, model ASAP 2010 from Micromeritics Inc., Norcross, GA. A summary of these results is given in Table 1.

The result showing the silicon map is shown in Fig. 1. The figure on the left shows a carbon nanotube bundle in bright field. The same bundle is shown in dark field through the energy filter centered on Si.[2] Clearly the silicon, and therefore SiCN, is uniformly covering the entire surface of the carbon nanotubes.

The weight fraction of SiCN was measured by TGA. These results are given in Fig. 2. The metallic residue left behind in the uncoated paper has been subtracted from the data. The difference in the residue between the uncoated and the coated paper, therefore, gives the weight fraction of SiCN since the SiCN remains intact at high temperatures.[1] Based on the amount of SiCN in the nanotube papers they are classified as U = uncoated, C1 = 10% residual SiCN and C2 = 50% residual SiCN. The weight fraction of SiCN, w_{SiCN}, can be converted into monolayers of SiCN, $\mathrm{ML}_{\mathrm{SiCN}}$, on the carbon nanotubes, assuming that SiCN covers the entire surface area of the nanotube structure, by the following relationship:

$$\mathrm{ML}_{\mathrm{SiCN}} = \frac{w_{\mathrm{SiCN}}}{1 - w_{\mathrm{SiCN}}} \times \frac{\mathrm{MW}_{\mathrm{C}}}{\mathrm{MW}_{\mathrm{SiCN}}} \times \left(\frac{\Omega_{\mathrm{SiCN}}}{\Omega_{\mathrm{C}}}\right)^{2/3} \quad (1)$$

where MW and Ω are the molecular weight and the molar volume/Avogadro's number respectively; the subscripts denote carbon in the nanotube and the SiCN molecule in the ceramic layer. Note that the weight fraction of carbon, $w_{\mathrm{C}} = 1 - w_{\mathrm{SiCN}}$.

SiCN is generally considered to be a pseudo-amorphous[8] compound, which forms over a range of compositions; therefore its density can vary.[1] Furthermore, the ultrathin, monolayer level, coatings being discussed here may have different physical properties than bulk materials. These issues mean that the molecular weight and the molar volume of SiCN in the coatings can be estimated only approximately. The chemical composition of bulk SiCN synthesized in our laboratory by the same process used to prepare the coating is $\mathrm{SiC}_{0.9}\mathrm{N}_{0.87}\mathrm{O}_{0.1}\mathrm{H}_{0.14}$. The compositions of the SiCN reported in literature vary widely, from $\mathrm{SiC}_{0.68}\mathrm{N}_{0.48}$ to $\mathrm{SiC}_{1.58}\mathrm{N}_{1}$, while the densities range from 2.2 to 2.6 g cm^{-3}. (While the residue obtained in the TGA was too small to be analyzed chemically, it is highly likely that its composition fell in this range.) The density of carbon is taken as 2.26 g cm^{-3} and the atomic volume as 0.0088 nm^3. With these values the $\mathrm{ML}_{\mathrm{SiCN}}$ is calculated to lie in the range 0.06–0.08 for C1 and 0.6–0.7 for C2.

The BET surface area analysis suggests that, in the sample C2, the nanotubes are nearly uniformly coated by SiCN. The surface to volume ratio will increase as the inverse of the effective diameter of the tubes. Assuming that the thickness of the SiCN monolayer is of the same order of magnitude as the wall thickness of the carbon nanotubes, it is to be expected that the surface area of C2 would be about one half the surface area of U. Indeed the BET measurements gave the following values: U, 544 m^2/g, C1, 490 m^2/g and C2, 290 m^2/g. It is curious that the addition of the coating to the nanotube structure made little change to the physical density of the samples: while U had a density of 0.6 g cm^{-3}, the coated samples had a density of 0.77 g cm^{-3}.

2.2. Electrical conductivity

The electrical conductivity of the specimens was measured by the four-point method at room temperature. The results are given in Table 1. The conductivity, σ, reduces progressively with increasing ceramic content. The sample C2 has 25% lower conductivity than the uncoated sample. The carbon nanotube paper is a stochastic, spaghetti-like structure. The conductivity of such a structure is likely to depend on the contact resistance at intertube interfaces as well as on the longitudinal conductivity along the length of the nanotube. The results from the coated samples suggest that SiCN reduces the overall conductivity by increasing the contact resistance between the nanotubes. However, the SiCN is not an insulator, otherwise the conductivity of the composite would have declined precipitously. The measurements of electrochemical capacitance, described below, further support the conductive nature of the SiCN coating.

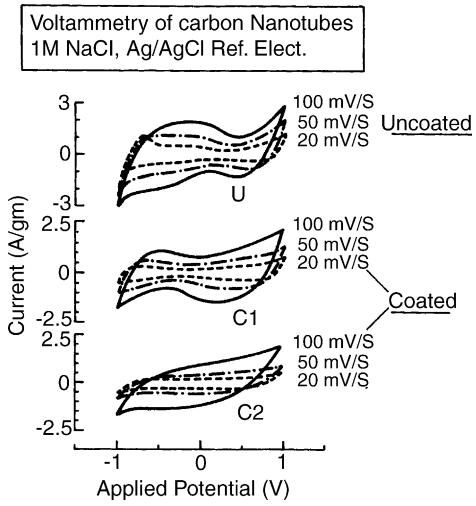

Fig. 3. Cyclic voltammogram of coated and uncoated nanotube papers in 1 M NaCl solution with triangular waveform at scan rates of 20, 50 and 100 mV/s.

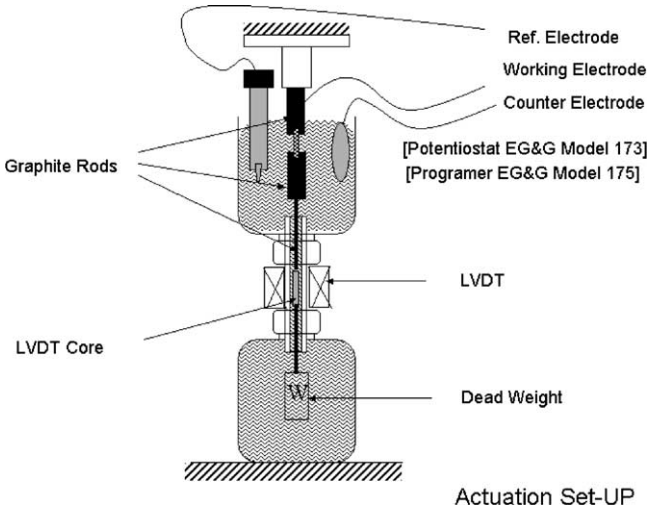

Fig. 5. Experimental set-up for measurement of actuation of nanotubes under dead weight load in a liquid electrolyte solution.

2.3. Electrochemical capacitance

The electrochemical capacitance was measured for each batch of coated and uncoated paper using potentiostat/galvanostat model 173 and programmer model 175, from EG&G PARC (Oak Ridge, TN). The potentiostat and programmer were used in unison to obtain cyclic voltammetry data at varied scan rate, recorded using a personal computer equipped with data acquisition hardware and Labview Software from National Instruments (Austin, TX). Ag/AgCl reference electrode was used for electrochemical measurements. A triangular waveform of voltage was used and corresponding current was recorded. To generate the cyclic voltammogram, current was plotted against the voltage and the hysteresis current at the midpoint of voltage scan was noted. Specific hysteresis current (hysteresis current/weight of the specimen) was plotted against the scan rate and the slope of this graph was used to calculate the capacitance of the material.[9] Fig. 3 shows the cyclic voltammogram for the specimens U, C1 and C2 in 1 M NaCl solution in water at scan rates of 20, 50 and 100 mV/S. Fig. 4 is the plot of the specific hysteresis current against the scan rate, slope of which gives the specific capacitance (per g), C_g, of the specimens. The values for C_g are given in Table 1.

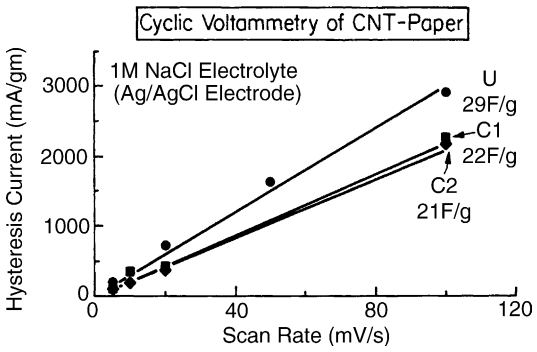

Fig. 4. Capacitance measurement in 1 M NaCl using the hysteresis currents from voltammograms.

The electrochemical capacitance of carbon structures is often expressed in terms of the capacitance per unit surface area, C_a, because different forms of carbon have been used as electrodes in supercapacitors.[10] The values for C_a in units of $\mu F/cm^2$ for the three specimens are also given in Table 1. Note that the C_a for the highly coated sample is 7.2 $\mu F/cm^2$ as compared to 5.3 $\mu F/cm^2$, that is, the coated sample has a 50% higher surface capacitance than the uncoated sample. These values are fairly typical for carbon structures.

2.4. Electrochemical actuation

A unique set-up was built to measure the influence of mean stress on the actuation strain. In this set-up a constant tensile load is applied to the specimen while it actuates under the cyclic voltage. The load is applied as a dead weight and is converted into a tensile stress by dividing it by the physical cross-sectional area of the specimen. The design of the set-up is shown schematically in Fig. 5. The electrolyte fills the lower chamber, which contains the dead weight, as well as the upper chamber containing the sample. The sample is held between a fixed graphite electrode and a moving graphite electrode, which is connected to the dead weight through an interconnecting tube. The core of the LVDT is in line of the load train and is immersed in the electrolyte in the region of the interconnecting tube. The LVDT transformer is placed outside this glass tube. The electrical system is the same potentiostat–programmer duo that was used for the capacitance measurements. Square wave potential pulses were applied to measure the electrochemically driven mechanical strain. The displacement of the specimen was measured by the LVDT. Data were collected and analyzed with the computerized data acquisition system similar to that used for the

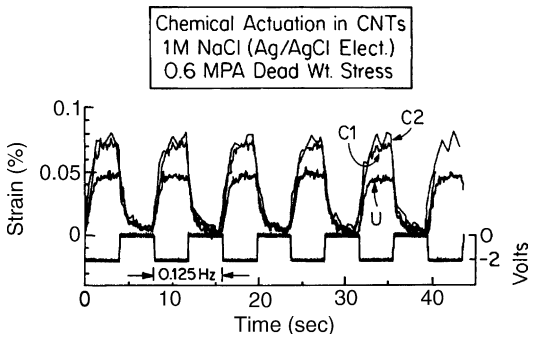

Fig. 6. Electrochemical actuation of coated and uncoated samples in 1 M NaCl solution under constant tensile stress of 0.6 MPa.

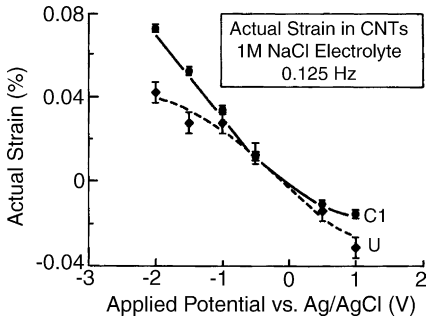

Fig. 8. The actuation strain as a function of the applied voltage for the coated and uncoated specimens. The data $V > +1$ V are not relevant because of the onset of electrolytic breakdown of 1 M NaCl.

capacitance measurement. The displacement was converted to strain using the gauge length of the specimen between the pull rods.

The results for short-term actuation are given in Fig. 6. They show the strain amplitude for the U, C1 and C2 samples for a square shaped voltage waveform fluctuating between 0 and −2 V. The measured values of the amplitude of the actuation strain are given in Table 1. These data, 0.05% strain for the uncoated sample, and 0.07 and 0.08% for the sample C1 and C2 were specific to these three samples. However, the actuation strain for a large number of samples (15 or more) was measured, and the range of the data obtained from these samples is quoted in the next column. These latter data show that actuation strain for the coated samples had less variability than the uncoated samples.

The results from long-term experiments on U and C2 are given in Fig. 7. The applied voltage was cycled between 0 and −2 V at a frequency of 0.125 Hz. A tensile stress of 0.5 MPa was used for the uncoated sample and 0.8 MPa for the coated sample. Same voltage cycle was applied to both samples. Note that the actuation in the coated sample is highly stable and reproducible whereas the uncoated sample continues to drift due to creep deformation. Such experiments can also be carried out under fixed displacement conditions but it is felt that the experiments reported here, under dead weight loading, can be interpreted more directly and simply. Further, such experiments can be carried out to measure the influence of the applied load on the actuation strain for a given voltage excursion; such experiments can provide information with regard to the "load lifting" capability of the actuation mechanism. The very limited data presented here shows the actuation strains in the two samples to be comparable even though the applied load is greater for the coated sample.

Finally, the data for actuation strain as a function of the applied voltage are given in Fig. 8. The coated sample shows better and more linear actuation response with the applied voltage. The voltage range is limited to $-2v < V < 1v$. Outside this range the water electrolyzes.

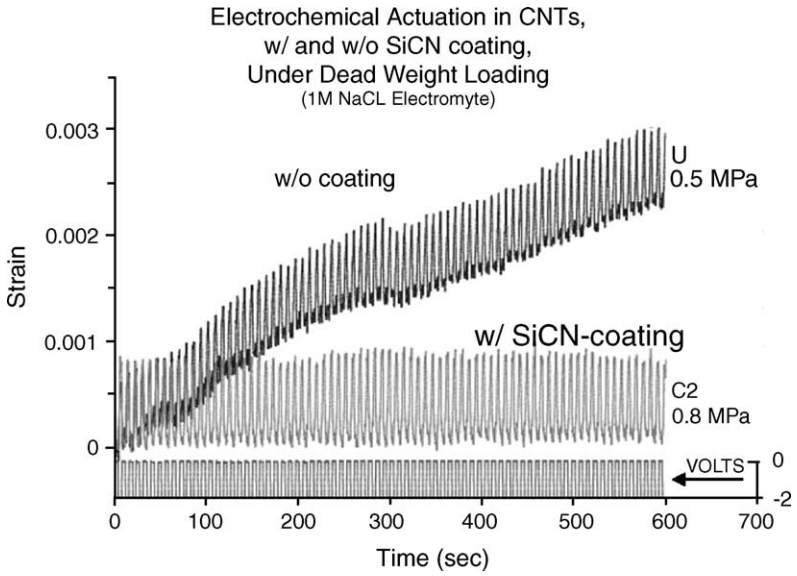

Fig. 7. Long-term actuation of uncoated and coated nanotube papers in 1 M NaCl electrolyte.

3. Discussion

The results presented in this paper raises the following questions:

(a) Why is the coating on the carbon nanotubes limited to about one monolayer of SiCN?
(b) Why is the surface specific capacitance unchanged despite the presence of the SiCN coating?
(c) Why is the actuation strain unchanged or even enhanced by the presence of the coating?

The first question arises from the results of an experiment where the amount of SiCN was increased and the weight fraction of the residue in TGA was measured. We discovered that the residue became constant at 50 wt.% fraction, that is, the maximum amount of SiCN that could be coated on the nanotubes was 50 wt.%. Interestingly this figure of 50% corresponds to about one monolayer of SiCN on nanotube surfaces. A likely explanation is that the first monolayer of the liquid precursor of SiCN self assembles on to the carbon surface and is strongly bonded to it; further addition of the precursor is weakly bonded to the wetted surface of the carbon nanotubes and volatilizes during pyrolysis.

The estimate of coverage of the nanotubes by SiCN, in monolayers, is given in Table 1. It ranges from 0.6 to 0.7 monolayers. Why is it less than one? Two possible reasons can be given. The first, which is more likely, is that a monolayer of the polymer precursor leaves behind SiCN, which is necessarily less than a monolayer because of some weight loss during pyrolysis. A second explanation is that the SiCN may not be able to penetrate all the intertube surfaces within all the bundles. Transmission electron microscopy studies suggest that the bundle diameter is typically 10 times the diameter of single wall carbon nanotubes. If only the surfaces of the bundles were being coated then the average monolayer coverage of SiCN would have been about 0.1 (since the surface to volume ratio is inversely proportional to the diameter); this possibility is unlikely since the coverage was much greater than 0.1 monolayer.

Before addressing questions (b) and (c) we briefly discuss the mechanism of electrochemical charging and actuation in carbon nanotube structures. The voltammetry data reported here measures the electrical charging of the carbon electrode. This process can be of two types: faradaic and nonfaradaic. The first case refers to electrochemical intercalation of the electrode; it often involves a redox reaction between the ions in the electrolyte and the electrode surface. The electrode stores electrical energy in the form of a charge by this intercalation process, like a battery, hence its called faradaic charging; intercalation of graphite with lithium ions is an example of faradaic charging. In the nonfaradaic capacitor, the mobile ionic charge in the electrolyte forms a double layer against the electronically conducting electrode, thus forming an electrostatic capacitor. In the ideal nonfaradaic capacitor, there is no electron transfer, of any kind, between the ions in the electrolyte and the electrons in the electrode; the capacitance is purely electrostatic. This capacitance can be huge because the thickness of the double layer is calculated to be just a few nanometers wide. The main way of distinguishing between faradaic and nonfaradaic behavior is the presence or the absence of sharp peaks in the voltammetry data. Sharp peaks imply faradaic, battery like behavior; they arise from the overpotential required for different kinds of redox reactions that may occur between the ions in the electrolyte and the electronic structure of the conducting electrode. A relatively smooth shape suggests a dominant nonfaradaic behavior.

Now let us consider the voltammetry data presented in Fig. 3. The data for the uncoated samples of carbon nanotubes is similar to those in the literature.[4] The curve shows peaks and valleys suggesting the presence of some sites in the carbon nanotube structure where a redox reaction with the electrolyte may be taking place. Interestingly, the highly coated sample, C2, is entirely devoid of such features, which suggests that the coated sample acted almost as an ideal nonfaradaic supercapacitor. Remarkably, the surface-specific capacitance of C2 was 7.2 $\mu F/cm^2$, one and a half times greater than the surface capacitance of the uncoated carbon nanotubes. This result is a good indication that the SiCN layer was electronically conducting, but without the reaction sites that are present in bare carbon nanotubes. *It is as if SiCN was itself a monolayer of carbon, but without the dangling bonds that are believed to be present in carbon nanotubes.*[11–14]

Faradaic and nonfaradaic supercapacitors are inherently mechanically actuating.[15] In the faradaic capacitors, the intercalation of ions into the electrode leads to volumetric expansion or contraction. In the nonfaradaic capacitors the injection of electrons into the lattice of the electrode can produce an expansion or contraction; in aromatic carbon the injection of one electron per carbon atom is expected to produce a strain of 0.096.[5] The uncoated nanotube paper is predominantly nonfaradaic; and the coated structure behaved like an ideal nonfaradaic capacitor. Therefore, the strains being measured must be understood in terms of the electron injection into the carbon structure by means of the double layer electrostatic capacitor.

The data, in Fig. 8 and Table 1, show that the actuation strain in the coated nanotubes was comparable, perhaps even somewhat higher, than the strain achieved in the uncoated structures. A key feature of these measurements was a much lower variability in the response in the coated samples, meaning that the data were more reproducible for the coated sample. This result is in line with the smoother voltammetry curves for the coated sample; the assumption being that the redox reactions seen in the uncoated samples[11–14] may also produce variability in the actuation behavior.

What may be the mechanism that can explain the unexpectedly good actuation response in the coated nanotube structures? Let us consider two scenarios: in one case the SiCN acts like an inert coating, and in the other case the coating actuates along with the carbon nanotubes. The idea

of an inert SiCN coating is untenable with the measurements of the capacitance: since the capacitance is not affected by the coating, it must be assumed that the coating is conducting and, therefore, the electronic charge is shared between the carbon nanotube and the coating (indeed the data suggest that the charge resides predominantly in the coating). It follows, that in the coated specimen the charge injected into the nanotubes, on a per carbon basis, is smaller than in the uncoated structure. Since the actuation strain is closely related to the charge injected per carbon atom, this view would suggest that the actuation strain w/ coating would be smaller than w/o coating. This inference is contrary to the experimental results. We infer that the charge injected into the SiCN is also producing an actuation strain. This view is not altogether surprising. Recent experiments with high surface area platinum have shown that electrolytic charging of the platinum electrode induces mechanical strain,[16] that is, most conducting materials are likely to show actuation if sufficient excess charge can be injected into them. It is, however, remarkable that the magnitude of the actuation strain is nearly the same with and without the SiCN coating; suggesting that SiCN may be acting like the carbon present in the nanotubes. Efforts to create self-standing high surface area structures from SiCN to investigate this possibility are underway. Also, in this context it is worth noting that NMR studies of SiCN have shown that it contains sp^2 coordinated carbon,[7] which may be present in the form of fragmented oriented graphene sheets.

4. Conclusions

The polymer-derived ceramic SiCN can be successfully and easily coated on to the surfaces of carbon nanotube structures. There is apparently a limit to the thickness of this coating that can be experimentally prepared; this limit is less than one monolayer of SiCN. The coating eliminates the broad redox peaks in the cyclic voltammograms seen in uncoated carbon nanotubes. The voltammetry data become smooth and highly reproducible in the presence of the SiCN monolayer.

The coating does not diminish either the supercapacitance behavior of the carbon nanotubes or the magnitude of the mechanical actuation induced by the electrolytic charge injection. This result is surprising—suggesting that the SiCN coating may itself be contributing to the actuation strain. The SiCN coating produces a ceramic-like bonding between the carbon nanotubes, adding mechanical robustness to the nanotube structure. Thus, the most important synergy between SiCN and the carbon nanotubes is the elimination of drift in the actuation strain without any degradation in the magnitude of the actuation strain in the carbon nanotube structures.

Acknowledgements

Authors would like to thank Prof. R.H. Baughman and his colleagues at the Nanotech Institute at the University of Dallas for numerous discussions in the course of this investigation. This research was supported by the Defense Advanced Projects Agency contracts N00173-99-2000 and MDA972-02-C-0005. The Colorado effort is a part of the DARPA program on Carbon Nanotubes at the University of Texas at Dallas. R.R. wishes to acknowledge support from the Council of Research and Creative Work at the University of Colorado at Boulder in the form of a Faculty Fellowship.

References

1. Kroke, E., Li, Y. L., Konetschny, C., Lecomte, E., Fasel, C. and Riedel, R., Silazane derived ceramics and related materials. *Mat. Sci. Eng. R.*, 2000, **26**(4–6), 97–199.
2. Shah, S. R., Cai, Y., Aldinger, F. and Raj, R., Nanoscopic ceramic welding of carbon nanotubes. *Adv. Mater.*, submitted for publication.
3. Rinzler, A. G., Huffman, C. B., Rodriguez-Macias, F. J., Nikolaev, P., Liu, J., Dai, H. *et al.*, Large-scale purification of single-wall carbon nanotubes: processes, product and characterization. *Appl. Phys. A*, 1998, **67**, 29–37.
4. Barisci, J. N., Wallace, G. G. and Baughman, R. H., Electrochemical characterization of single-walled carbon nanotube electrodes. *J. Electrochem. Soc.*, 2000, **147**(12), 4580–4583.
5. Gartstein, Y. N., Zakhidov, A. A. and Baughman, R. H., Charge-induced anisotropic distortions of semiconducting and metallic carbon nanotubes. *Phys. Rev. Lett.*, 2002, **89**(4), 45503.
6. Baughman, R. H., Cui, C., Zakhidov, A. A., Iqbal, Z., Barisci, J. N., Spinks, G. M. *et al.*, Carbon nanotube actuators. *Science*, 1999, **284**(5418), 1340–1344.
7. Trassl, S., Motz, G., Rossler, E. and Ziegler, G., Characterization of free-carbon phase in precursor derived SiCN ceramics. *J. Non-Cryst. Solids*, 2001, **293–295**, 261–267.
8. Kleebe, H.-J., Suttor, D. and Motz, G., Microstructure evolution and crystallization behavior of polymer-derived Si–C–N monoliths: a TEM study. In *Precursor Derived Ceramics*, ed. J. Bill, F. Wakai and F. Aldinger. Wiley-VCH, Weinhein, Germany, 1999, pp. 113–131.
9. Gileadi, E., *Electrode Kinetics for Chemists, Chemical Engineers and Materials Scientists*. VCH, New York, 1993 [pp. 213–223].
10. Conway, B. E., *Electrochemical Supercapacitors*. Kluwer Academic, New York, 1999.
11. Curran, S., Davey, A. P., Coleman, J., Dalton, A., McCarthy, B., Maier, S. *et al.*, Evolution and evaluation of polymer nanotube composite. *Synth. Met.*, 1999, **103**(1–3), 2259–2262.
12. Kavan, L., Rapta, P., Dunsch, L., Bronikowski, M. J., Willis, P. and Smalley, R. E., Electrochemical tuning of electronic structure of single-walled carbon nanotubes: in-situ Raman and vis-NIR Study. *J. Phys. Chem. B*, 2001, **105**, 10764–10771.
13. An, K.-H., Jeon, K.-K., Heo, J.-K., Lim, S.-C., Bae, D.-J. and Lee, Y.-H., High capacitance supercapacitor using a nanocomposite electrode of single-walled carbon nanotube and polypyrrole. *J. Electrochem. Soc.*, 2002, **149**(8), A1058–A1062.
14. Tahhan, M., Truong, V.-T., Spinks, G. M. and Wallace, G. G., Carbon nanotube and polyaniline composite actuators. *Smart Mater. Struct.*, 2003, **12**, 626–632.
15. Baughman, R. H., Conducting polymer artificial muscles. *Synth. Met.*, 1996, **78**, 339–353.
16. Weissmuller, J., Viswanath, R. N., Kramer, D., Zimmer, P., Wurschum, R. and Gleiter, H., Charge-induced reversible strain in a metal. *Science*, 2003, **300**(5617), 312–315.